JOURNAL OF COMPUTATIONAL PHYSICS 17, 384–400 (1975)

A Fast Method for Nuclear Coupled-Channels Calculations Including Coulomb Excitation

L. D. TOLSMA

Eindhoven University of Technology, Department of Physics, Cyclotron laboratory, Eindhoven, the Netherlands

Received September 11, 1974

To reduce the computation time in nuclear coupled-channels calculations including Coulomb excitation, the applicability of Gordon's numerical method has been investigated to the integration range beyond the range of the nuclear potential. It turns out that a considerable reduction of computation time can be obtained. The larger the integration range and the relative wave number, pertinent to a given reaction process and reaction energy, the larger is this reduction. This is illustrated by two test cases dealing with α and ^{16}O scattering near the Coulomb barrier. Consequently, although the method is sometimes also of considerable advantage in the case of scattering of light particles, it seems to be especially suitable to heavy ion scattering problems.

1. INTRODUCTION

The inclusion of the contribution of Coulomb excitation in coupled-channels calculations of nuclear scattering problems often increases the computation time considerably. To reduce this time we have investigated the applicability of a method for solving systems of coupled linear second-order differential equations, introduced by R. G. Gordon in connection with atomic and molecular scattering and bound state problems [1, 2]. For most collisions between atoms and ions at thermal energies, the de Broglie wavelength associated with the relative motion is short as compared to the long range of the interatomic potential. This range can then be divided into intervals which are sufficiently small to approximate the potential matrix by a linearly varying reference potential matrix and which on the other hand contain a sufficient number of de Broglie wavelengths. This enables one to write the general solution vector in e.g., the classically allowed region as a linear combination of two rapidly oscillating Airy functions with slowly varying coefficient vectors. An important advantage of Gordon's method is connected with the fact that part of the numerical procedure is independent of energy. Apart from a possible decrease of computation time at a single scattering

energy [3], an additional amount of time is thus saved when the calculation is repeated at a slightly different energy.

In Section 2, we give a concise formulation of Gordon's method. In Section 3, the application of Gordon's method to nuclear scattering problems is discussed. To study this applicability, the method has been implemented in Tamura's code JUPITOR. In the resulting code JUPIGOR, the integration range is divided into a part up to the radius where the nuclear interaction has died out and a large part where only the Coulomb interaction operates. From preliminary calculations it appeared that Gordon's method is not efficient over the first part: the step size has to be taken too small. This part is therefore dealt with by a conventional step-by-step method. Subsequently, the remaining integration range is divided into steps such that the Coulomb interaction matrix is linearized, up to a few percent over one step. Here Gordon's method turns out to be very efficient and to reduce computation time considerably.

In Section 4, we present the results of our study on the 11.5, 16.5, 21.5 MeV ^{122}Te(α, α')^{122}Te [12] and 39, 44, 49 MeV ^{58}Ni(^{16}O, ^{16}O')^{58}Ni [13] inelastic scattering problems. Preliminary results of our investigation on the 10–16 MeV ^{114}Cd(α, α')^{114}Cd inelastic scattering problem have been published elsewhere [14].

2. A Concise Formulation of Gordon's Method

The Schrödinger equation for the partial wave radial function in potential scattering is, in conventional notation,

$$\left\{\frac{d^2}{dr^2} + k^2 - \frac{2m}{\hbar^2} V(r) - \frac{l(l+1)}{r^2}\right\} \psi(r) = 0. \tag{2.1}$$

This equation can be rewritten into the form

$$(d^2\psi/dr^2) + \{k^2 - U(r)\}\,\psi = 0. \tag{2.2}$$

Consider some interval of the integration range with the midpoint at radius $\bar{r}$. Although in Gordon's method several forms can be used for the reference potential, we follow him in choosing a linear one of the form

$$U_0(r) = \bar{U}(\bar{r}) + (r - \bar{r})(dU/dr)|_{r=\bar{r}}, \tag{2.3}$$

where $\bar{U}$ is the average value of the potential over the interval. Using (2.3) as potential in (2.2) gives us the Airy functions Ai and Bi as a set of two linearly independent solutions. As shown by Gordon these functions can be efficiently evaluated numerically. The general reference solution may now be written as

$$\psi_0(r) = Ai[\alpha(\beta + r)]\,a + Bi[\alpha(\beta + r)]\,b, \tag{2.4}$$

with the constants

$$\alpha = \left(\frac{dU}{dr}\bigg|_{r=\bar{r}}\right)^{1/3}, \qquad \beta = \frac{\bar{U}(\bar{r}) - k^2}{dU/dr\,|_{r=\bar{r}}} - \bar{r}. \tag{2.5}$$

The constant coefficients a and b are determined by conditions of continuity at the interval boundaries. For instance, if they would be adapted to the value and derivative of the exact solution $\psi(r)$ at the "left-hand" boundary r_l,

$$a = \pi\{Bi'[\alpha(\beta + r_l)]\,\psi(r_l) - \alpha^{-1}\,Bi[\alpha(\beta + r_l)]\,\psi'(r_l)\}, \tag{2.6a}$$

$$b = \pi\{\alpha^{-1}\,Ai[\alpha(\beta + r_l)]\,\psi'(r_l) - Ai'[\alpha(\beta + r_l)]\,\psi(r_l)\}, \tag{2.6b}$$

where the prime denotes differentiation with respect to the argument.

Including the difference between the true potential and the reference potential one obtains corrections $\Delta a(r)$ and $\Delta b(r)$ to the coefficients a and b. The solution of the Schrödinger Eq. (2.2) can now be approximated by the reference solution (2.4) plus a correction term

$$\psi(r) \approx Ai[\alpha(\beta + r)]\{a + \Delta a(r)\} + Bi[\alpha(\beta + r)]\{b + \Delta b(r)\}, \tag{2.7}$$

where the varying coefficients, to first order in $[U(r) - U_0(r)]$ are given by

$$\Delta a(r) = -\pi \int_{r_l}^{r} Bi[\alpha(\beta + r')]\{U(r') - U_0(r')\}\,\psi_0(r')\,dr', \tag{2.8a}$$

$$\Delta b(r) = \pi \int_{r_l}^{r} Ai[\alpha(\beta + r')]\{U(r') - U_0(r')\}\,\psi_0(r')\,dr'. \tag{2.8b}$$

These coefficients remain small as long as the reference potential is a good approximation to the true potential. Thus, in the classically allowed region the solution (2.7) has been written as a linear combination of two rapidly oscillating Airy functions with slowly varying coefficients. The integrals in (2.8) can be evaluated analytically.

In the case of n coupled equations the differential operator and k^2 in (2.2) stand for diagonal $(n \times n)$ matrices while the potential is in general a nondiagonal $(n \times n)$ matrix $\mathbf{U}(r)$. To obtain a reference potential matrix a similarity transformation is performed which reduces $\mathbf{U}(\bar{r})$ to diagonal form

$$\mathbf{X}^{-1}\mathbf{U}(\bar{r})\,\mathbf{X} = \mathrm{diag}(\lambda_c), \tag{2.9}$$

where $\mathbf{X}$ is the transformation matrix and λ_c are the eigenvalues. In other words $\mathbf{U}(\bar{r})$ has been transformed from a *free* basis into a *local* basis such that it is diagonal. As reference potential matrix the following diagonal matrix is chosen

$$\mathbf{U}_0(r) = [\mathbf{X}^{-1}\bar{\mathbf{U}}(\bar{r})\,\mathbf{X}]_{\mathrm{diag}} + (r - \bar{r})[\mathbf{X}^{-1}(d\mathbf{U}/dr)|_{r=\bar{r}}\,\mathbf{X}]_{\mathrm{diag}}, \tag{2.10}$$

where $\bar{\mathbf{U}}(\bar{r})$ is the average value of the potential matrix over the interval and the subscript "diag" means that only the diagonal elements are retained. With this diagonal matrix the set of reference equations becomes uncoupled and the Airy functions are again the linearly independent exact solutions. Writing the Airy functions in diagonal matrix form, the general reference solution vector in the *local* basis is given by

$$\boldsymbol{\psi}_0 = \mathbf{Ai}\,\mathbf{a} + \mathbf{Bi}\,\mathbf{b}. \tag{2.11}$$

The constant coefficient vectors **a** and **b** are once more determined by boundary conditions like (2.6). The solution vector of the coupled equations may now be approximated by

$$\boldsymbol{\psi} \approx \mathbf{Ai}(\mathbf{a} + \boldsymbol{\Delta}\mathbf{a}) + \mathbf{Bi}(\mathbf{b} + \boldsymbol{\Delta}\mathbf{b}), \tag{2.12}$$

where the varying coefficient vectors are determined by

$$\boldsymbol{\Delta}\mathbf{a} = -\pi \int_{r_l}^{r} \mathbf{Bi}\{\mathbf{U} - \mathbf{U}_0\}\, \boldsymbol{\psi}_0\, dr', \tag{2.13a}$$

$$\boldsymbol{\Delta}\mathbf{b} = \pi \int_{r_l}^{r} \mathbf{Ai}\{\mathbf{U} - \mathbf{U}_0\}\, \boldsymbol{\psi}_0\, dr'. \tag{2.13b}$$

The continuity condition for the solution vector in the free basis leads to a relation between the local solution vector in interval p and that in interval $p + 1$, both taken at the common boundary point:

$$\boldsymbol{\psi}_{p+1} = \mathbf{X}_{p+1}^{-1}\mathbf{X}_p\boldsymbol{\psi}_p \equiv \mathbf{T}_p\boldsymbol{\psi}_p\,. \tag{2.14}$$

Note that the following quantities are independent of energy:

the diagonalized potential matrix $\mathbf{X}^{-1}\bar{\mathbf{U}}\mathbf{X}$,
the transformed derivative potential matrix $\mathbf{X}^{-1}(d\mathbf{U}/dr)\,\mathbf{X}$,
the transformation matrix $\mathbf{T}_p$.

These quantities can therefore be used at other values of the energy, which turns out to save more than half of the computation time.

The general solution vector can be written as a linear combination of n independent solution vectors. These solution vectors can be collected as the columns of a solution matrix $\boldsymbol{\Psi}$. The component c of the vector s (solution) is denoted by ψ_{cs}. Suppose that the components in the solution vectors are arranged in order of decreasing local relative kinetic energy. Integrating through a classically forbidden region, the components with negative kinetic energy will in general consist of an exponentially growing and an exponentially decreasing part. The former is responsible for a tendency to destroying the initially taken linear indepen-

dence of the solution vectors. To maintain this linear independence, the solution matrix can be stabilized by an unitary transformation such that the exponentially growing components below the diagonal with local negative kinetic energy are eliminated. In this way a stable solution matrix $\tilde{\Psi}$ is obtained

$$\tilde{\Psi}^* = \Psi^* \mathscr{U}, \tag{2.15}$$

in terms of the original solution matrix Ψ. The unitary matrix $\mathscr{U}$ can be chosen [4] as a product of elementary unitary Hermitian matrices: $\mathbf{P}_n\mathbf{P}_{n-1} \ldots \mathbf{P}_c \ldots$, in which c runs over the components with local *negative* kinetic energy and with

$$\mathbf{P}_c = \mathbf{I} - 2\mathbf{w}_c\mathbf{w}_c^{\dagger}. \tag{2.16}$$

The unit column vector $\mathbf{w}_c$ with n components can be constructed from row c of Ψ:

$$2K\mathbf{w}_c^{\dagger} = (\psi_{c1}^*, \psi_{c2}^*, \ldots, \psi_{cc}^* + S\psi_{cc}^*/|\psi_{cc}|, 0, \ldots, 0), \tag{2.17}$$

where K and S are defined as positive constants, given by the expressions

$$S^2 = \sum_{s=1}^{c} \psi_{cs}\psi_{cs}^*, \qquad 2K^2 = S^2 + S|\psi_{cc}|. \tag{2.18}$$

It can easily be shown that the solution matrix $\tilde{\Psi}$ obtained has vanishing elements below the diagonal in the rows c up to and including n, while the corresponding elements of the derivative of $\tilde{\Psi}$ become small. If on the other hand a different choice is made for $\mathbf{w}_c$ by replacing ψ_{cs} by ψ'_{cs} in Eq. (2.17), the abovementioned results for $\tilde{\Psi}$ and $\tilde{\Psi}'$ are interchanged. Clearly, it is possible to eliminate the exponentially growing solution by means of the linear combination $k_c\psi_{cs} + \psi'_{cs}$. The wave number k_c is defined as $(|\lambda_c|)^{1/2}$ in terms of one of the negative eigenvalues λ_c in Eq. (2.9).

In Gordon's method [1] the solution vectors are real. In view of our preference for the use of complex solution vectors in Section 3, we have given the abovementioned formulae in an adapted notation. Furthermore, we note that in Gordon's code an approximation to $[\mathbf{X}^{-1}\bar{\mathbf{U}}(\bar{r})\,\mathbf{X}]_{\text{diag}}$ in Eq. (2.10) is used. In Section 3 this approximation is not made. We use in Eq. (2.9) $\bar{\mathbf{U}}(\bar{r})$ instead of $\mathbf{U}(\bar{r})$.

3. The Application of Gordon's Method to Nuclear Scattering Problems

The Calculational Procedure

The coupled-channels formalism for inelastic scattering in nuclear physics has been discussed extensively in the literature [5–8]. This formalism leads to a set of

coupled differential equations for the radial wave functions u_{Il}^J of the following form

$$\left[\frac{\hbar^2}{2m}\left(\frac{d^2}{dr^2} - \frac{l(l+1)}{r^2}\right) + (E - \epsilon_I) - \frac{z_1 z_2 e^2}{r} + V^{\text{opt}}\right] u_{Il}^J(r) = \sum_{I'l'} V_{Il;I'l'}^J(r)\, u_{I'l'}^J(r), \tag{3.1}$$

assuming a spinless projectile. Here J, l and I denote the total angular momentum, the orbital angular momentum and the spin of the target nucleus in the state with excitation energy ϵ_I, respectively. The coupling potential is denoted by $V_{Il;I'l'}^J$, the optical model potential by V^{opt}, whereas z_1 and z_2 are the charge numbers of the projectile and target nucleus, respectively. The total angular momentum J, its projection on the z-axis and the parity are good quantum numbers.

If n is the number of coupled equations (3.1) for a given J, the solution satisfying the usual boundary conditions [6] can be written as a linear combination of n independent regular solutions $u_{Il}^{J(\nu)}$

$$\sum_{\nu=1}^{n} a^{(\nu)} u_{Il}^{J(\nu)} \underset{r\to\infty}{\sim} (2l+1)^{1/2}\, e^{i\sigma_l}\left[\delta_{II_i}\delta_{ll_i} F_l + \left(\frac{k_i}{k}\right)^{3/2} C_{I_i l_i;Il}^J \{G_l{}^J + iF_l\}\right], \tag{3.2}$$

where G_l and F_l are the irregular and regular Coulomb wave functions and σ_l the partial-wave Coulomb phase shift. The subscript i refers to the initial channel. A similar set of equations holds for the derivatives of the respective functions and together with Eq. (3.2) they supply the matching and normalization conditions. The calculated matrix elements $C_{I_i l_i;Il}^J$ are used in the calculation of the elastic and inelastic scattering amplitudes.

To study the applicability of Gordon's method, it has been implemented in Tamura's code JUPITOR [9]. In the resulting code JUPIGOR, the integration range is divided into a part up to the radius where the nuclear interaction has died out, to be called the coupling radius r_{cp} and a large part up to the matching radius r_m where only the Coulomb interaction operates.

From preliminary calculations for a single channel case with a complex nuclear potential, it appeared that Gordon's method is not efficient up to the radius r_{cp}. The step size has to be taken too small, because the nuclear potential varies too fast over this range to be efficiently linearized. This part is therefore dealt with by a conventional method with a step size of 0.1 to 0.2λ [10], where λ is the de Broglie wavelength. In JUPITOR the step-by-step Störmer method is used for this purpose. Subsequently, we divide the remaining integration range into steps such that the potential is linearized up to a few per cent over one step. In the next subsection the procedure followed in choosing the step sizes will be dealt with.

Choosing Step Sizes

Taking a perturbation potential matrix $[\mathbf{U}(r) - \mathbf{U}_0(r)]$ which is quadratic in r on the diagonal and linear in r for the off-diagonal elements, the perturbation integrals (2.13) can be evaluated analytically. Notwithstanding this, the calculation of these first-order corrections to the reference solution needs extended matrix multiplications. As a consequence, the calculation of the solution (2.12) requires about two or three times as much computational effort as does the calculation of the reference solution (2.11) alone. In view of this it is useful to avoid the calculation of the perturbation integrals in cases where this is possible.

In Gordon's method the step size is taken such that the perturbation integrals are small enough to keep the accuracy of the reference solution at some required level. For some potential and total angular momentum this requires the calculation of these integrals once; for subsequent calculations at different energies, with the same potential and total angular momentum, the reference solution can then be calculated efficiently using the same intervals and applying the energy independent matrices following Eq. (2.14) of Section 2.

In our application of Gordon's method we prefer to prescribe the step size without the calculation of the perturbation integrals. Over the integration range $r_{cp} < r < r_m$ the potential of each uncoupled equation of set (3.1) has a radial dependence of the form $2\eta k r^{-1} + l(l+1)\, r^{-2}$, where η is the Coulomb parameter. Preparatory calculations have shown that in the case of an uncoupled equation a sufficient accuracy of the final results can be obtained by choosing the step sizes

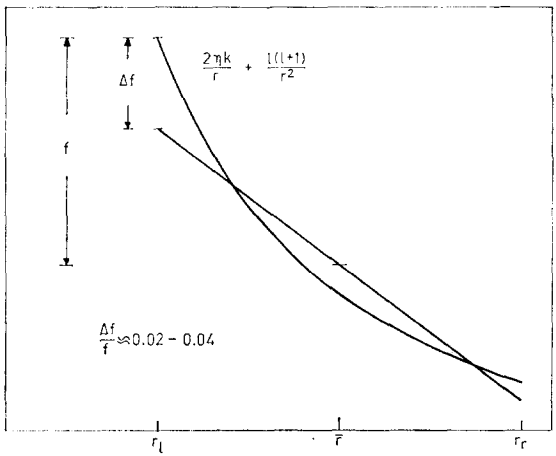

FIG. 1. The step sizes over the integration range from r_{cp} to r_m are chosen by linearizing the potential up to a few percent over one step.

such that over one step the maximal deviation of the actual potential with respect to the linearized potential equals a few percent of the difference between the actual potential and the average potential (see Fig. 1). In the case of coupled equations it is evident that coinciding intervals have to be chosen in all channels of the same coupled J set. The step size is determined according to the abovementioned method, applied to a similar potential form $2\eta kr^{-1} + l(l+1)\, r^{-2}$, in which now an average value of l over the coupled channels has been taken into account. For the test cases to be dealt with in Section 4 the first steps have a size of about 1 fm, the last few about 8 fm, depending on the value of r_m.

The radial region around the classical turning points of the individual equations deserves special attention, because the coupling between the equations is most effective here. This complication occurs for such high J values that some or all of the turning points are beyond r_{cp}. In the region of turning points more rigorous linearizing conditions are imposed.

In this way we can work with the reference solution avoiding the calculation of the perturbation integrals (2.13). For subsequent calculations with the same total angular momentum and Coulomb interaction but with a different energy and/or nuclear interaction the reference solution can be evaluated using the same step sizes and applying again the energy independent matrices following Eq. (2.14).

4. Results and Discussion

In this section the results of two test cases will be presented. In both cases the multiple excitation of a "vibrational" nucleus with one-phonon and two-phonon triplet states is considered. The excitation is induced by inelastic scattering of alpha and ^{16}O particles, respectively, near the Coulomb barrier. The code JUPIGOR allows independent variation of each of the optical potential deformation parameters β, involved in the coupling of the levels considered. In addition, the corresponding reduced electric multipole matrix elements can be introduced independently. In view of the purpose of this paper, however, we prefered to consider the following simple choice. The coupling potential has been expanded up to and including the first order in the deformation. A purely harmonic vibrational model is assumed. As a consequence, the deformation parameters β_{02}, β_{20}, β_{22} and β_{24}, defined by Tamura [11], have been taken equal, whereas $\beta'_{00} = \beta'_{02} = \beta'_{04} = 0$. The common β value is given below. Some of the calculated C-matrix elements for alpha and ^{16}O scattering have been collected in Tables I and II, respectively. In Fig. 2 the reduction of computation time for Gordon's method compared with Störmer's method, is given as a function of the matching radius r_m for a total angular momentum value $J = 5$.

Multiple Excitation of ^{122}Te *by* 11.5, 16.5, *and* 21.5 MeV ^{4}He

In this case, the Coulomb parameter and wave number are about 8.0 and 1.7, respectively. The optical model parameters are: $V = 250$ MeV, $W = 37.6$ MeV, $r_v = r_w = r_c = 1.333$ fm, $a_v = a_w = 0.582$ fm. The abovementioned deformation parameters are taken equal to 0.15.

Calculations were carried out for several total angular momentum J values. However, we have concentrated our attention in this article on $J = 5$ and 30, because the results for these two J values turn out to be representative for the general properties of low and high J values. Furthermore, calculations were performed for several r_m values distributed between 25 and 200 fm. It appears that in most practical calculations for this reaction with energies near the Coulomb barrier, the contribution of Coulomb excitation to the C-matrix elements can only be neglected if r_m is chosen equal to about 100 fm or larger. In the following we shall confine ourselves to such r_m values. In addition, to study the extent of linear independence of the solution vectors, calculations were also carried out in the $J = 30$ case for different r_{cp} values.

In Table I the C-matrix elements are presented for $J = 5$ and 30 at laboratory energies of 16.5 and 21.5 MeV. The rows containing the C-matrix elements calculated with our code JUPIGOR are denoted by G, those with Tamura's code JUPITOR by T. The results have been obtained with r_{cp} and r_m values of 15 and 100 fm, respectively.

First, we discuss the $J = 5$ ($I_i = 0$; $l_i = 5$) results for $E_{\text{lab}} = 16.5$ MeV ($G - 1$, $T - 1$, $T - 2$, $T - 3$) and $E_{\text{lab}} = 21.5$ MeV ($G - 2$, $T - 4$). Row $G - 1$ contains the C-matrix elements, obtained with a step size of 0.10 fm for Störmer's method up to r_{cp} and 33 steps according to Gordon's method for the remaining integration up to r_m. The rows $T - 1$, $T - 2$, and $T - 3$ contain the elements calculated with step sizes of 0.05, 0.10 and 0.20 fm, respectively, for Störmer's method over the whole integration range. Comparing $G - 1$ with $T - 1$, we see that in most C-matrix elements a 3-figure correspondence is obtained. Variations of of r_m beyond 100 fm lead to changes in the C-matrix elements $G - 1$ of a fraction of 1 %. To get an indication of the computational efficiencies we have compared $G - 1$ with $T - 2$, the latter results being almost identical to $T - 1$. For $r_m = 100$ fm this gives a reduction of the computation time by a factor of about 9 (Fig. 2). Row $G - 2$ contains the C-matrix elements obtained at at $E_{\text{lab}} = 21.5$ MeV using the same intervals from r_{cp} to r_m as in $G - 1$ and applying the energy independent matrices as expressed in Section 2 (following Eq. (2.14)), which already have been calculated for $G - 1$. In this way the computation time is reduced by a total factor of about 20 (Fig. 2). As evident from Table I, the correspondence of $G - 2$ with $T - 4$ is satisfactory. A similar correspondence is obtained at an energy of 11.5 MeV. These results have not been presented.

Next, we discuss the $J = 30$ ($I_i = 0$; $l_i = 30$) results for $E_{\text{lab}} = 16.5$ MeV ($G - 3$, $T - 5$, $T - 6$, $T - 7$) and $E_{\text{lab}} = 21.5$ MeV ($G - 4$, $T - 8$). Row $G - 3$ contains the C-matrix elements obtained with a step size of 0.20 fm for Störmer's part ($r_{cp} = 15$ fm, $r_m = 100$ fm). This step size can be taken relatively large because of the monotonous behaviour of the solution vector up to r_{cp}. Gordon's method needs in this case 44 steps. The rows $T - 5$, $T - 6$ and $T - 7$ contain the elements calculated with step sizes of 0.05, 0.10 and 0.20 fm, respectively. Comparing these results the correspondence can be considered as satisfactory except for some elements, particularly the elastic channel and the $I_f = 4$, $l_f = 32{,}34$ elements. Calculations for r_m beyond 100 fm give rise to variations of the $G - 3$ elements within one per cent, apart from some elements which show variations of a few percent. The C-matrix elements of the elastic channel and the small elements for $I_f = 4$, $l_f = 32{,}34$, which are not expected to contribute significantly to cross sections, show larger relative variations, but remain of the same order of magnitude.

The abovementioned discrepancy in the C-matrix element of the elastic channel can be understood by considering that the elastic component of the solution vector in Eq. (3.2), divided by $(2l + 1)^{1/2} \exp(i\sigma_l)$, corresponds at this high J value with the regular Coulomb wave function F_l in about four figures. Consequently, the relatively small value of the C-matrix element is obtained by subtracting two quantities, which agree up to about four figures, and is rather sensitive to small variations in the elastic component of the solution vector. However, we believe that in most practical calculations this discrepancy has no consequences.

The discrepancy for $I_f = 4$, $l_f = 32{,}34$ cannot be explained on this basis: the accuracy of the C-matrix elements of the inelastic channels is more directly related to the accuracy of the inelastic components of the solution vector. We believe that the $T - 5$ and $T - 6$ values for these C-matrix elements are too large due to a numerical instability in the Störmer procedure, originating from a tendency of the solution vectors to become linearly dependent for high angular momenta. To confirm this we have carried out addition calculations for different r_{cp} values ($r_m = 100$ fm).

For r_{cp} values up to about 15 fm, it turns out that in all C-matrix elements a 3 à four-figure correspondence is obtained, whereas for $r_{cp} = 20$ fm some C-matrix elements begin to show agreement to within two-figures. The correspondence for the r_{cp} values larger than 20 fm remains acceptable, except for the $I_f = 4$, $l_f = 32{,}34$ elements. We note that for $J = 30$ the radial region of the classical turning points of the individual equations lies between $r \approx 21$ and $r \approx 26$ fm. For $r_{cp} = 25$ fm the $I_f = 4$, $l_f = 32{,}34$ elements still have the same order of magnitude, but they deviate more and more for r_{cp} values of 30 and 35 fm, lying in the classically allowed region, especially when a step size of 0.05 fm is taken over the integration range up to r_{cp}. In this case they become of the same order of magnitude as in the case $T - 5$ of Table I.

TABLE I

A Sample $C^{J}_{I_i l_i; I_f l_f}$ for $^{122}Te(\alpha,\alpha')$ with target states $0^+ - 2^+(0.564) - 0^+(1.357) - 2^+(1.257) - 4^+(1.180)$

$I_i = 0$ $l_i = 5$	I_f l_f															
	0	5	2	3	2	5	2	7	0	5	2	3	2	5	2	7
E_{lab}=16.5 MeV	(-1)	(0)	(-2)	(-1)	(-1)	(-1)	(-1)	(-2)	(-3)	(-3)	(-2)	(-2)	(-3)	(-3)	(-3)	(-4)
G-1[a] .100[b] 33[c]	[r].631	[r].144	.714	.563	.275	-.234	-.213	-.996	-.876	-.837	.212	.199	-.718	-.705	.266	.197
T-1[d] .050[e]	.629	.144	.714	.563	.275	-.234	-.213	-.997	-.876	-.837	.212	.199	-.718	-.705	.267	.192
T-2 .100	.628	.144	.715	.563	.275	-.234	-.213	-.997	-.877	-.838	.212	.199	-.719	-.706	.267	.196
T-3 .200	.581	.143	.820	.560	.272	-.234	-.214	-.997	-.759	-.780	.212	.123	-.626	-.652	.282	-.072
E_{lab}=21.5 MeV	(-1)	(0)	(-1)	(-1)	(-2)	(-1)	(-1)	(-2)	(-2)	(-1)	(-2)	(-2)	(-2)	(-2)	(-2)	(-2)
G-2 .100 33	-.412	.440	.291	.170	.875	-.270	-.348	-.982	.383	-.112	.653	.622	.233	-.652	-.834	-.202
T-4 .100	-.412	.440	.291	.170	.874	-.270	-.348	-.981	.382	-.112	.653	.622	.233	-.652	-.834	-.201

	I_f l_f									
	4	1	4	3	4	5	4	7	4	9
E_{lab}=16.5 MeV	(-2)	(-2)	(-3)	(-2)	(-3)	(-3)	(-3)	(-3)	(-3)	(-3)
G-1 .100 33	-.464	-.119	.176	.120	-.449	-.552	.383	.132	-.275	-.495
T-1 .050	-.464	-.119	.176	.120	-.450	-.551	.384	.132	-.277	-.406
T-2 .100	-.464	-.119	.176	.120	-.450	-.553	.384	.133	-.277	-.406
T-3 .200	-.466	-.092	.173	.122	-.377	-.469	.413	.101	-.274	-.408
E_{lab}=21.5 MeV	(-1)	(-3)	(-2)	(-2)	(-2)	(-2)	(-2)	(-2)	(-4)	(-2)
G-2 .100 33	-.118	-.447	.522	.586	.363	-.620	-.345	-.252	.124	.840
T-4 .100	-.118	-.442	.522	.586	.363	-.620	-.345	-.252	.159	.840

$I_i = 0$ $l_i = 30$	I_f l_f															
	0	30	2	28	2	30	2	32	0	30	2	28	2	30	2	32
E_{lab}=16.5 MeV	(-3)	(-3)	(-1)	(-3)	(-2)	(-2)	(-3)	(-2)	(-4)	(-4)	(-4)	(-4)	(-5)	(-6)	(-4)	(-5)
G-3[a] .200[b] 44[c]	.342	.158	.108	.424	.559	-.309	.813	-.131	.346	.108	.569	.823	-.289	-.162	.107	-.200
T-5[d] .050[e]	.052	.155	.107	.410	.559	-.309	.821	-.129	.346	.108	.559	.824	-.276	-.477	.153	.247
T-6 .100	-.032	.156	.107	.408	.559	-.309	.800	-.130	.342	.108	.559	.824	-.298	-.480	.109	-.565
T-7 .200	-4.65	.177	.107	.317	.556	-.313	.794	-.130	.342	.104	.565	.818	-.287	-.409	.113	-.242
E_{lab}=21.5 MeV	(-3)	(-3)	(-1)	(-2)	(-2)	(-2)	(-2)	(-2)	(-4)	(-4)	(-4)	(-3)	(-5)	(-5)	(-4)	(-5)
G-4 .200 44	.034	.222	.118	.166	.834	-.291	.168	-.168	.539	.485	.438	.156	-1.01	-.625	.240	.730
T-8 .100	-.217	.224	.118	.166	.833	-.292	.169	-.168	.537	.485	.454	.157	-.954	-.616	.245	.781

	I_f l_f									
	4	26	4	28	4	30	4	32	4	34
E_{lab}=16.5 MeV	(-4)	(-3)	(-4)	(-4)	(-4)	(-4)	(-4)	(-5)	(-5)	(-5)
G-3 .200 44	-.125	.178	.412	.804	.369	.210	.105	-.012	.194	-.137
T-5 .050	-.149	.177	.415	.801	.369	.208	-.002	1.21	71.0	-76.3
T-6 .100	-.149	.177	.415	.801	.369	.209	.119	-.258	-3.65	-4.03
T-7 .200	-.134	.177	.420	.796	.369	.206	.104	-.046	.511	-5.40
E_{lab}=21.5 MeV	(-4)	(-3)	(-4)	(-3)	(-4)	(-4)	(-4)	(-4)	(-5)	(-5)
G-4 .200 44	-.891	.208	.245	.141	.530	.844	.214	.102	.596	-.629
T-8 .100	-.675	.218	.255	.141	.530	.644	.214	.111	6.97	-2.42

[a] Rows containing JUPIGOR results. [b] Step size for Störmer's method up to r_{cp}. [c] Number of steps from r_{cp} to r_m.
[d] Rows containing JUPITOR results. [e] Step size for Störmer's method over the whole integration range.
[f] Left entries mean: $ReC^J = .831_{10}{}^{-1}$, right entries mean: $ImC^J = .144_{10}{}^{0}$, where additional exponents have been added between brackets above the columns.

TABLE II

A Sample $C^{J}_{I_i l_i; I_f l_f}$ for $^{58}Ni(^{16}O, ^{16}O')$ with target states $0^+ - 2^+(1.454) - 0^+(2.943) - 2^+(2.775) - 4^+(2.459)$

$I_i = 0$ $l_i = 5$	I_f l_f															
	0	5	2	3	2	5	2	7	0	5	2	3	2	5	2	7
E_{lab}=44.0 MeV	(0)	(0)	(-1)	(-1)	(-1)	(-1)	(-1)	(-1)	(-3)	(-2)	(-2)	(-2)	(-2)	(-2)	(-2)	(-2)
G-1[a] .050[b] 32[c]	[f].118	[g].380	.493	.246	-.264	-.272	.102	.407	-.886	.909	.343	-.587	-.218	.545	.285	-.516
T-1[d] .025[e]	.116	.380	.494	.246	-.264	-.272	.102	.408	-.873	.906	.343	-.588	-.218	.545	.284	-.517
T-2 .050	.118	.380	.495	.244	-.265	-.272	.103	.407	-.848	.906	.341	-.588	-.216	.545	.282	-.517
T-3 .100	.095	.382	.520	.160	-.301	-.222	.104	.380	-.485	.882	.243	-.615	-.129	.556	.197	-.538
E_{lab}=49.0 MeV	(-1)	(0)	(-2)	(-1)	(-2)	(-1)	(-2)	(-1)	(-2)	(-2)	(-2)	(-2)	(-2)	(-4)	(-2)	(-2)
G-2 .050 32	-.373	.505	.894	.204	-.260	-.189	-.340	.217	-.821	.188	.766	-.319	-.482	-.760	.415	.228
T-4 .050	-.376	.505	.909	.204	-.268	-.189	-.336	.217	-.819	.191	.764	-.321	-.481	-.572	.415	.226

	I_f l_f									
	4	1	4	3	4	5	4	7	4	9
E_{lab}=44.0 MeV	(-2)	(-2)	(-2)	(-2)	(-2)	(-2)	(-2)	(-2)	(-2)	(-2)
G-1 .050 32	-.768	.366	.560	-.226	-.537	.203	.504	-.212	-.539	.181
T-1 .025	-.769	.366	.560	-.226	-.537	.203	.504	-.212	-.539	.182
T-2 .050	-.767	.368	.559	-.227	-.536	.205	.503	-.213	-.538	.184
T-3 .100	-.686	.468	.506	-.301	-.487	.276	.453	-.280	-.491	.256
E_{lab}=49.0 MeV	(-1)	(-2)	(-2)	(-3)	(-2)	(-2)	(-2)	(-2)	(-2)	(-2)
G-2 .050	-.117	.234	.751	-.222	-.570	-.168	.320	.331	.103	-.438
T-4 .050	-.117	.238	.750	-.250	-.570	-.158	.321	.300	.101	-.438

$I_i = 0$ $l_i = 30$	I_f l_f															
	0	30	2	28	2	30	2	32	0	30	2	28	2	30	2	32
E_{lab}=44.0 MeV	(-2)	(-2)	(-1)	(-1)	(-2)	(-1)	(-2)	(-2)	(-3)	(-3)	(-2)	(-3)	(-5)	(-3)	(-3)	(-4)
G-3[a] .200[b] 36[c]	.605	.326	.479	-.200	-.200	-.214	-.678	-.187	-.256	-.616	.154	-.868	-.283	-.234	-.222	-.295
T-5[d] .025[e]	.600	.325	.479	-.199	-.200	-.213	-.667	-.184	-.256	-.614	.154	-.865	.086	-.233	-.221	-.276
T-6 .050	.459	.324	.479	-.200	-.205	-.213	-.667	-.182	-.257	-.612	.153	-.868	.029	-.233	-.221	-.271
T-7 .100	-7.66	.916	.438	-.266	-.513	-.205	-.677	-.079	-.330	-.556	.136	-1.05	-3.18	-.225	-.216	.038
E_{lab}=49.0 MeV	(-1)	(-2)	(-1)	(-1)	(-2)	(-1)	(-2)	(-2)	(-3)	(-2)	(-2)	(-4)	(-3)	(-3)	(-3)	(-3)
G-4 .200 36	.110	.496	.606	-.108	.472	-.267	-.705	-.467	.191	-.102	.267	-.720	.174	-.233	-.276	-.235
T-8 .050	.122	.496	.605	-.106	.472	-.266	-.701	-.464	.191	-.102	.266	-.620	.178	-.233	-.273	-.233

	I_f l_f									
	4	26	4	28	4	30	4	32	4	34
E_{lab}=44.0 MeV	(-2)	(-2)	(-2)	(-3)	(-3)	(-3)	(-3)	(-3)	(-4)	(-4)
G-3 .200 36	.200	.422	.191	-.323	.121	-.812	-.243	-.149	-.796	.587
T-5 .025	.201	.420	.190	-.322	.119	-.811	-.243	-.146	-.783	.595
T-6 .050	.202	.419	.189	-.327	.117	-.810	-.243	-.145	-.799	.586
T-7 .100	.254	.379	.179	-.579	.001	-.800	-.254	-.107	-.673	.672
E_{lab}=49.0 MeV	(-3)	(-2)	(-2)	(-3)	(-3)	(-2)	(-3)	(-3)	(-3)	(-4)
G-4 .200 36	.403	.628	.268	.720	.729	-.101	-.213	-.384	-.151	.211
T-8 .050	.391	.624	.267	.728	.728	-.101	-.213	-.382	-.150	.183

[a] Rows containing JUPIGOR results. [b] Step size for Störmer's method up to r_{cp}. [c] Number of steps from r_{cp} to r_m.
[d] Rows containing JUPITER results. [e] Step size for Störmer's method over the whole integration range.
[f] Left entries mean: $ReC^J = .118_{10}{}^{0}$, right entries mean: $ImC^J = .380_{10}{}^{0}$, where additional exponents have been added between brackets above the columns.

Looking at the *solution vectors*, it turns out that for r_{cp} values of about 5 fm and larger the Störmer procedure generates some solution vectors, which show a tendency to become linearly dependent. We conclude, however, that by using Gordon's stabilization transformation in the classically forbidden region for sufficiently small r_{cp} values, this tendency can be suppressed, which then leads to reliable values of the C-matrix elements.

The Störmer procedure used in Tamura's code does not contain a facility to maintain linear independence. However, we believe that in principle it is possible to apply Gordon's stabilization procedure to the Störmer method. In this case the potential matrix needs only to be diagonalized to determine the arrangement of the components in the solution vectors in order of decreasing relative kinetic energy. It is not necessary to transform the solution vectors into a local basis. Presumably, stabilization is only needed in a few points of the classically forbidden region. We have not realized these ideas in the Störmer procedure to stabilize the solution vectors below r_{cp}. The reason is that in general and also in our test cases, the linear dependence enters only for high J values. However, note that in our code JUPIGOR r_{cp} has been chosen such that the nuclear potential can be neglected outside r_{cp}. In the first instance one may be inclined to conclude from this that it is less meaningful to take r_{cp} smaller than 15 fm, the value of r_{cp} which has been taken for the results in the table. For high J values, however, the nuclear potential no longer contributes significantly to the C-matrix elements. (This is already the case for $J \approx 15$.) In these cases a small r_{cp} value can be recommended to guarantee the linear independence of the solution vectors, as well as for reasons of computational efficiency. For practical cross section calculations it is therefore advantageous to take r_{cp} for the high J values considerably below 15 fm, e.g., 1 fm, or even smaller. In JUPIGOR this is actually done.

The C-matrix elements in row $G - 4$ are calculated by using the energy independent matrices, which already have been determined in $G - 3$. The correspondence with $T - 8$ is satisfactory, except for the abovementioned discrepancies. About a similar correspondence is obtained at an energy of 11.5 MeV.

Multiple Excitation of ^{58}Ni *by* 39, 44 *and* 49 MeV ^{16}O

This case has a Coulomb parameter and wave number of about 21 and 4.5, respectively. The optical model parameters are: $V = 22.69$ MeV, $r_v = 1.30$ fm, $a_v = 0.533$ fm, $W = 2.35$ MeV, $r_w = 1.37$ fm, $a_w = 0.375$ fm, and $r_c = 1.25$ fm [13]. The deformation parameters are taken equal to 0.18. The values of r_{cp} and r_m have again been taken as 15 and 100 fm, respectively. In Table II the C-matrix elements are presented as before for $J = 5$ and 30 at laboratory energies of 44 and 49 MeV.

We discuss now the $J = 5$ ($I_i = 0$, $l_i = 5$) results for $E_{lab} = 44$ MeV ($G - 1$, $T - 1$, $T - 2$, $T - 3$) and $E_{lab} = 49$ MeV ($G - 2$, $T - 4$). Comparing $G - 1$

with $T - 1$ we see that in most C-matrix elements a three-figure correspondence is obtained. However, the comparison with $T - 2$ gives only small discrepancies and may be used to determine the reduction of the computation time. For $r_m = 100$ fm this reduction is about a factor of 18 (Fig. 2). The C-matrix elements of row $G - 2$ at $E_{lab} = 49$ MeV have again been obtained by applying energy independent matrices. The reduction of the computation time is now a total factor of about 42 (Fig. 2). The agreement with $T - 4$ is satisfactory. A similar agreement is evident from the results at an energy of 39 MeV, which have been left out in Table II.

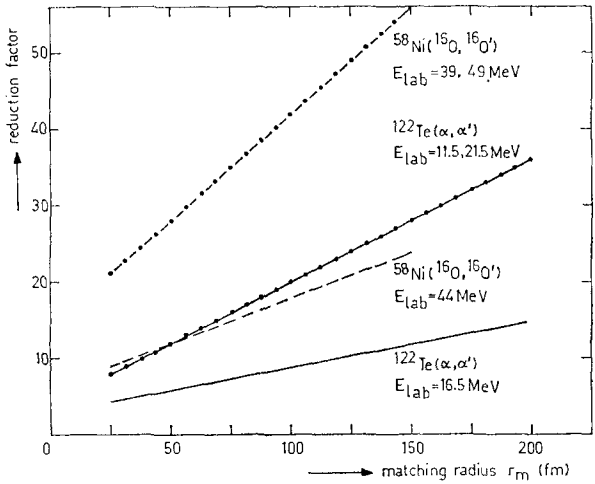

FIG. 2. Reduction factor of computation time for Gordon's method compared with Störmer's method, applied to the integration range from r_{cp} to r_m for a total angular momentum value $J = 5$. The solid and dashed curves represent the results of alpha and oxygen particles scattering, respectively. The dotted curves represent the results obtained by applying energy independent matrices already calculated for a different energy.

Finally, considering the $J = 30$ ($I_i = 0$, $l_i = 30$) results for $E_{lab} = 44$ MeV ($G - 3$, $T - 5$, $T - 6$, $T - 7$) and $E_{lab} = 49$ MeV ($G - 4$, $T - 8$) similar conclusions can be drawn as in the preceding $J = 30$ case. Note, however, that the type of discrepancy observed for some C-matrix elements is absent here.

5. CONCLUSION

In describing a nuclear reaction process including Coulomb excitation by means of a coupled-channels calculation, the analysis often involves the solution of a large set of coupled linear second-order differential equations. It turns out that a con-

siderable reduction of computation time can be obtained by applying Gordon's numerical method, especially if the calculation is to be carried out for various energies and/or optical model parameter sets. The larger the integration range and the relative wave number, pertinent to the reaction process, the larger is this reduction. Consequently, although the method is also of considerable advantage in some light particle scattering cases, it seems to be especially suitable to heavy ion scattering problems. Furthermore, a comparison of the results in this paper with those recently published by the present author [14], indicates that the reduction factor increases also with the dimension of the set of coupled equations to be solved.

ACKNOWLEDGMENTS

The author is thankful to Dr. B. J. Verhaar for his helpful conversations and critical reading of the manuscript, as well as to the computer centre of the Eindhoven University of Technology, where the calculations were carried out on a Burroughs 6700 computer.

REFERENCES

1. R. G. GORDON, *J. Chem. Phys.* **51** (1969), 14.
2. R. G. GORDON, *in* "Methods in Computational Physics: 10, Atomic and Molecular Scattering" (B. Alder, S. Fernbach, and M. Rotenberg, eds.), p. 81, Academic Press, New York, 1971.
3. A. C. ALLISON, *J. Comput. Phys.* **6** (1970), 378.
4. J. H. WILKINSON, "The Algebraic Eigenvalue Problem," pp. 152, 233, Oxford University Press, London, 1965.
5. B. BUCK, *Phys. Rev.* **130** (1963), 712.
6. T. TAMURA, *Revs. Mod. Phys.* **37** (1965), 679.
7. U. SMILANSKY, *Nucl. Phys. A* **112** (1968), 185.
8. K. ALDER AND H. K. A. PAULI, *Nucl. Phys. A* **128** (1969), 193.
9. T. TAMURA, Oak Ridge National Laboratory Report No. ORNL-4152 (1967); H. REBEL AND G. W. SCHWEIMER, Kernforschungszentrum Karlsruhe Report No. KFK-1333 (1971).
10. P. E. HODGSON, "The Optical Model of Elastic Scattering," p. 43, Oxford University Press, London, 1963.
11. T. TAMURA, *Prog. Theor. Phys. Supplement No.* **37–38** (1966), 383.
12. M. SAMUEL AND U. SMILANSKI, Proc. Int. Conf. Reac. Complex Nuclei, Nashville, (R. L. Robinson, *et al.*, Eds.), Vol. I, p. 188, North-Holland Publ. Co., Amsterdam, 1974.
13. P. R. CHRISTENSEN, I. CHERNOV, E. E. GROSS, R. STOKSTAD, AND F. VIDEBAECK, *Nucl. Phys. A* **207** (1973), 433.
14. L. D. TOLSMA, Proc. Int. Conf. Nucl. Phys., Munich, (J. de Boer and H. J. Mang, Eds.), Vol. I, p. 385, North-Holland Publ. Co., Amsterdam, 1973.